Challenging Glass Conference Proceedings – Volume 10 – June 2026 – Louter, Bos & Belis (Eds.)
International Conference on the Architectural and Structural Application of Glass
Challenging Glass Conference 10 – 15-17 June 2026 – TU Delft – The Netherlands

Hardness-Adapted Borate Glass as Wear Indicator

Michelle Grüne [a], Jan Kückelheim [a], Michael Marré [b], Bernd Ahrens [a,c], Stefan Schweizer [a,c]

a Department of Electrical Engineering, South Westphalia University of Applied Sciences, Lübecker Ring 2, 59494 Soest, Germany, gruene.michelle@fh-swf.de, kueckelheim.jan@fh-swf.de, ahrens.bernd@fh-swf.de, schweizer.stefan@fh-swf.de

b Department of Mechanical Engineering, South Westphalia University of Applied Sciences, Frauenstuhlweg 31, 58644 Iserlohn, Germany, marre.michael@fh-swf.de

c Department of Physical Metrology, Fraunhofer Institute for Molecular Biology and Applied Ecology IME, Lübecker Ring 2, 59494 Soest, Germany, bernd.ahrens@ime.fraunhofer.de, stefan.schweizer@ime.fraunhofer.de

Abstract

Glass, in particular borate glass, is not only a very robust and hard material, but also offers good solubility for lanthanide ions. The lanthanide ions serve as luminescence centres in the glass system and emit a characteristic luminescence when excited by light in the ultraviolet/blue spectral range. The triply ionized lanthanide europium (Eu^{3+}) enables a very intense red luminescence that is clearly visible even under strong contaminated conditions. Such luminescent glasses can be integrated into metallic tools for non-destructive, optical wear measurements. For this, the glass is incorporated into tool areas that are subject to abrasive wear. A key challenge of this approach is to match the hardness of the glass to that of the tool steel so that both have the same wear rate. In borate glass, this can be achieved by changing the ratio of network modifier to network former. Deep, converging holes are drilled into the tool and filled with an Eu^{3+}-activated phosphor. As abrasion increases, the distance between the holes decreases. Measuring the distance between the red luminescent holes provides information about the degree of wear. The approach enables predictive maintenance, prevents tool failures and reduces production downtime, thereby increasing process reliability.

Keywords

Borate Glass, Hardness, Luminescence, Europium, Wear Indicator

Article Information

- Digital Object Identifier (DOI): 10.47982/cgc.10.674
- Published by Challenging Glass, on behalf of the author(s), at Stichting OpenAccess.
- Published as part of the peer-reviewed Challenging Glass Conference Proceedings, Volume 10, June 2026, 10.47982/cgc.10
- Editors: Christian Louter, Freek Bos & Jan Belis

1. Introduction

Non-destructive wear measurement enables continuous component monitoring during operation, eliminating the need for machine shutdowns or component disassembly (Ogunnowo 2020). These testing methods deliver real-time condition data, forming the foundation of contemporary condition-based maintenance approaches that demonstrably reduce unplanned downtime and enhance asset reliability (Daily 2017). The integration of such methods into Industry 4.0 ecosystems has gained substantial momentum, with advanced frameworks now incorporating sensorised tooling, edge analytics, and digital twin architectures for real-time health monitoring (Aminzadeh 2023, Moreira 2020). Emerging technologies including AI-driven anomaly detection systems, autonomous measurement platforms, and innovative sensing modalities such as millimetre-wave radar and smartphone-based optical metrology are rapidly expanding the application spectrum of non-destructive testing (Swain 2022).

Contemporary non-destructive testing encompasses well-established techniques including ultrasonic inspection, demonstrated for autonomous condition monitoring of rotating components in wind turbines and other critical machinery (Galarza-Urigoitia 2019), alongside x-ray and computed tomography methods recognized for volumetric defect detection in safety-critical applications (Aminzadeh 2023). These approaches facilitate early identification of progressive wear phenomena through near-real-time monitoring capabilities, thereby substantially improving equipment availability and operational safety (Diamanti 2021). Industry implementations have documented considerable cost reductions and enhanced availability through the elimination of inspection-related downtime and disassembly requirements (Daily 2017). Across safety-critical sectors, which include energy infrastructure, aerospace manufacturing, petrochemical operations, and mechanical engineering, continuous wear monitoring supported by edge-deployed AI models and digital twin frameworks has become integral to modern production and maintenance paradigms (Chehrehzad 2024).

A promising approach to expanding the range of non-destructive wear detection methods is to incorporate lanthanide-doped glass fibres into a tool or component. The fibres can then be excited in the ultraviolet and blue spectral range to show an intense luminescence in the visible spectral range. The intensity of the luminescence can be measured by a detector and provides direct information about the current state of wear.

The advantage of borate glass investigated here is that its composition allows the mechanical properties to be adjusted. In this way, the hardness of the glass can always be adapted to that of the material, ensuring that it experiences the same wear. In this work, two different borate glass systems, namely lithium aluminoborate and barium borate glass with different compositions are investigated for their luminescence properties as well as their mass density and Vickers hardness.

2. Experimental details

2.1. Samples

The series of borate glasses investigated is based on the network former boron oxide (B_2O_3 from Alfa Aesar, 99 % purity). The network modifier for the LiAlB and the BaB glass series are lithium oxide (Li_2O from Alfa Aesar, 99.5 % purity) and barium oxide (BaO from Sigma-Aldrich, 97 % purity), respectively. As pure lithium borate glass suffers from hygroscopicity, the property modifier aluminium oxide (Al_2O_3 from Alfa Aesar, 99 % purity) is added at the expense of boron oxide to improve the chemical stability

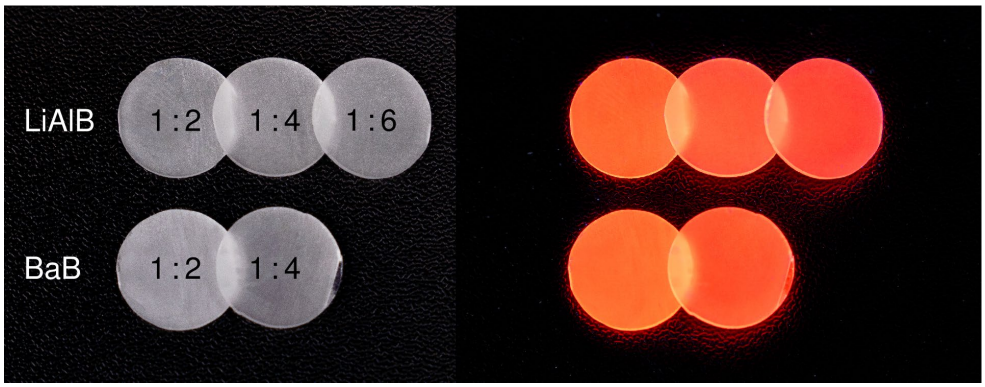

Fig. 1: Eu3+-doped LiAlB and BaB glasses under ambient light (left) and under ultraviolet excitation (right).

of the glass (Fan 2020). For optical activation, europium oxide (Eu_2O_3 from Alfa Aesar, 99.99 % purity) is added at the expense of all other components. The ratio between network modifier and network former is varied, while the Eu_2O_3 concentration is kept constant. The nominal chemical compositions of the investigated glasses are listed in Table 1.

For the preparation of the samples (Figure 1), the chemicals are mixed and heated in a platinum gold crucible (Pt/Au 95/5) to a temperature of 1100 °C and kept there for 2.5 hours. Subsequently, the melt is poured onto a 450 °C (LiAlB) and 550 °C (BaB) pre-heated brass block, which is below the corresponding glass transition temperature (Rimbach 2018). To eliminate residual internal stress, the glass is held at this temperature for 3 hours before being cooled down to room temperature at a rate of 2 K/min. The samples are produced in a circular shape with a diameter of 20 mm. They are ground to a thickness of approximately 4 mm and subsequently polished to optical quality.

2.2. Setup

The mass density of each glass is determined by the Archimedes' principle with a density determination kit for an analytical balance (Mettler Toledo, XS105DU). For each value, ten measurements are performed. The resulting arithmetic mean is listed in Table 1. The experimental error amounts to ±0.005 g/cm^3. The investigation of the Vickers hardness, *HV*, is done with a fully-automated hardness testing machine (ZwickRoell EMCO-TEST, DuraScan 70 G5) having a load range between 0.000 25 kp and 62.5 kp. A square-based pyramidal diamond indenter with an angle of 136° between the opposing side faces is used for indentation. The indentations are performed in accordance with DIN EN ISO 6507.

Table 1: Nominal composition, mass density, and Vickers hardness of the LiAlB and BaB glasses investigated. The experimental error of the density values amounts to ±0.005 g/cm^3, that of the hardness values to ±2 %.

ratio	composition in mol%					Eu^{3+}	density	*HV*
	Li_2O	BaO	B_2O_3	Al_2O_3	Eu_2O_3	in at.%	in g/cm^3	in MPa
1 : 2	33.00		59.40	6.60	1.00	0.46	2.361	537
1 : 4	19.80		71.28	7.92	1.00	0.43	2.234	417
1 : 6	14.14		76.37	8.49	1.00	0.42	2.189	376
1 : 2		33.00	66.00		1.00	0.50	3.555	577
1 : 4		19.80	79.20		1.00	0.45	2.900	479

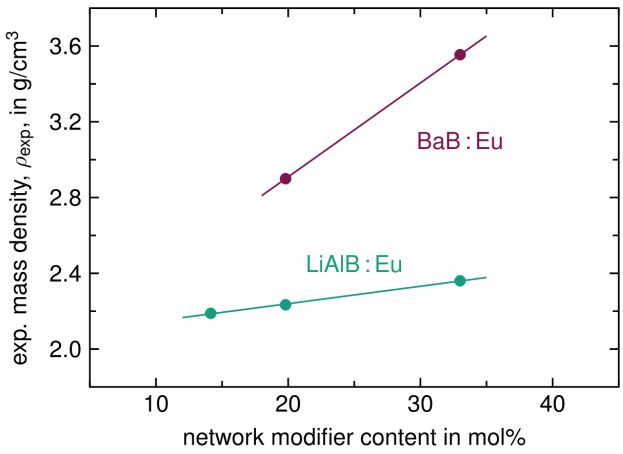

Fig. 2: Mass density of Eu3+-doped LiAlB and BaB glass with varying network modifier content.

Transmittance measurements are performed with a UV-Vis-NIR spectrophotometer (Agilent Technologies, Cary 5000). Photoluminescence (PL) emission spectra as well as external quantum efficiency (EQE) are measured with an absolute PL quantum yield measurement system (Hamamatsu, C9920-02G). This system comprises a xenon lamp (150 W) for excitation, which is connected via a monochromator to a 3.3-inch integrating sphere, and a photonic multi-channel analyser (Hamamatsu, PMA-12) for detection.

3. Experimental results

3.1. Mass density

The measured mass density shows a significant increase upon changing the modifier-to-former ratio in favour of the network modifier (Figure 2). This change is in particular noticeable for the network modifier BaO as the molar mass of BaO (153.33 g/mol) is significantly higher than that of Li_2O (29.88 g/mol). In case of LiAlB glass, the density also increases even though the molar mass of B_2O_3 is larger than that of Li_2O. This shows how the amount of the network modifier influences the formation of boron units in the network which then impacts the arrangement and structure of the network (Shelby 2005). The mass density values range between 2.189 g/cm^3 (LiAlB – 1 : 6) and 3.555 g/cm^3 (BaB – 1 : 2). For both systems, the mass density increases linearly with increasing amount of network modifier. The mass density of BaB glass is always higher than that of LiAlB glass. All mass density values are collected in Table 1.

3.2. Vickers hardness

The hardness of the glasses is tested at a load of 2 kp (19.6133 N) to indent the optical polished glass surface. Each indentation leaves a square imprint in the glass. The hardness testing is done on each sample with 15 indentations. The two diagonals, d_1 and d_2, of the indentation are measured to calculate the hardness via

$$HV = \frac{0.1891\,F}{d^2} \tag{1}$$

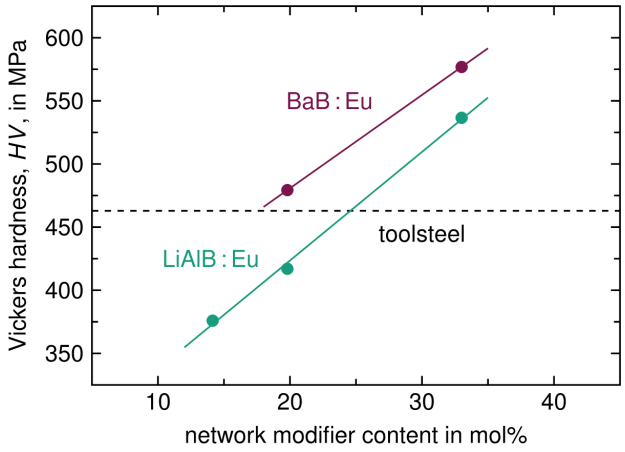

Fig. 3: Vickers hardness of Eu^{3+}-doped LiAlB and BaB glass with varying network modifier content at a load of 2 kp.

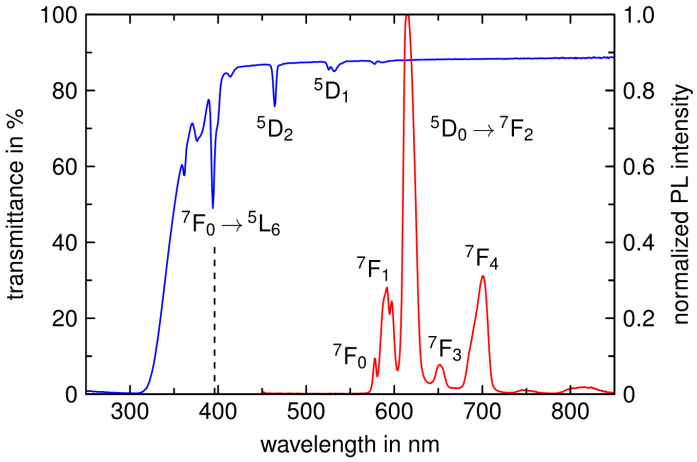

Fig. 4: Transmittance and PL spectra of the Eu3+-doped BaB glass sample with a modifier-to-former ratio of 1 : 4. The emission spectrum (red curve) is recorded under 396-nm excitation.

with the indentation load, F, in N and the mean of the two diameters, d_1 and d_2, in mm (Anstis 1981, Barlet2015). The resulting values are plotted versus the network modifier content, as shown in Figure 3. The hardness tests result in values between 376 HV 2 (LiAlB – 1 : 6) and 577 HV 2 (BaB – 1 : 2). For the same modifier-to-former ratio, BaB is always harder than LiAlB. For both glass systems, the glass with a modifier-to-former ratio of 1 : 2 achieves the highest hardness values of 537 HV 2 and 577 HV 2 for LiAlB and BaB, respectively. A linear dependence of the hardness versus the modifier content is found. All values are added to Table 1.

3.3. Photoluminescence

Figure 4 (blue curve) shows exemplarily the transmittance of the Eu_2O_3-doped BaB glass with a modifier-to-former ratio of 1 : 4. The spectrum shows absorption bands in the ultraviolet/blue spectral range which are typical for Eu^{3+} (Dieke 1963). The bands at 531 nm, 464 nm, 414 nm, and 363 nm correspond to transitions from the ground state $^7F_0$ to the excited states ^5D_J (J = 1, 2, 3, 4), respectively. Additional bands are ascribed to transitions from the ground state to the excited states $^5L_6$, $^5G_2$, and $^5H_4$ at 396 nm, 383 nm, and 319 nm, respectively. The strongest absorption is obtained for the $^7F_0$ to $^5L_6$ transition at 396 nm.

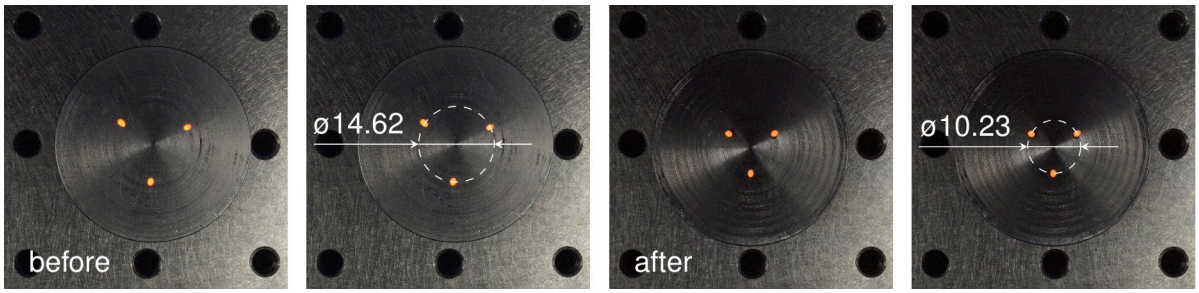

Fig. 5: Three holes are drilled at an angle of 45° into a round steel test specimen with a diameter of 38 mm. For proof of principle, the holes are subsequently filled with an Eu3+-doped luminescent powder. The photos show the test specimen under ultraviolet excitation before and after wear. The circumcircle of the luminescent dots is indicated by a dashed line.

The emission spectrum (red curve) is recorded under 396-nm excitation, which brings the system into the excited state $^5L_6$. From there, the system relaxes non-radiatively to the excited state $^5D_0$ and then radiatively to the ground states $^7F_0$, $^7F_1$, $^7F_2$, $^7F_3$, and $^7F_4$, resulting in emission bands at 580 nm, 592 nm, 613 nm, 652 nm, and 700 nm respectively. The PL emission of the other four glasses under study looks very similar (not shown). The electric dipole transition $^5D_0$ to $^7F_2$ is hypersensitive to variations in crystal symmetry. The high intensity of this transition indicates the amorphous nature of the matrix material with low inversion symmetry for the Eu^{3+} ion. Emissions in the blue spectral range (from higher energy levels) are quenched due to the high maximum phonon frequency in borate glass (Blasse 1994). For the LiAlB and BaB glasses investigated, the emission intensity differs only slightly, i.e., all systems are promising candidates as luminescent wear indicator.

3.4. Test specimen

The idea to use luminescent glass as wear indicator involves the integration of luminescent glass fibres into forging tools for direct, spatially resolved wear monitoring. The glass fibres are inserted in such a way that they are gradually exposed as abrasive wear progresses. When optically excited, the exposed fibre sections emit a characteristic light signal that can be detected with spatial resolution using an optoelectronic unit.

For proof of principle, three holes are drilled at an angle of 45° into a round steel test specimen and filled with a luminescent powder (Figure 5). The drill holes lie at the edges of an equilateral triangle; the circumcircle of this triangle is indicated by a dashed line. The more the test specimen experiences wear, the smaller the diameter of the circumcircle becomes. As the holes are drilled at an angle of 45°, the difference between the radius of the circumcircle before and after wear gives a direct measure for the wear ($\tan(45°) = 1$), i.e.,

$$\Delta x_{\text{wear}} = \frac{r_{\text{before}} - r_{\text{after}}}{\tan(45°)} = r_{\text{before}} - r_{\text{after}}. \tag{2}$$

In case of Figure 5, the wear amounts to 2.20 mm.

The fibre is produced in such a way that its hardness is specifically adapted to the tool steel. This means that the fibre wears synchronously with the tool matrix and provides valid measurements. Compared to existing force, temperature, or imaging methods, the system offers a direct, quantifiable, and robust wear indicator inside the tool and thus a non-destructive method, preventing any downtime.

4. Conclusion

The optical activation of LiAlB and BaB glass with Eu^{3+} ions results in a very promising luminescent wear indicator for use in tools and components. The mechanical hardness of the glass can be adapted to that of toolsteel by changing the modifier-to-former ratio accordingly. The measured Vickers hardness depends linearly on the network modifier content. The higher the modifier content the harder the glass. Maximum hardness values of 537 HV 2 (LiAlB) and 577 HV 2 (BaB) are achieved.

The photoluminescence properties are investigated under 396-nm excitation. The glasses show a very intense red luminescence which is typical for Eu^{3+}. The emission is clearly visible even under very soiled conditions. The luminescent material is filled into three drill holes of a test specimen resulting in a position shift of the luminescent holes under wear due to the 45° geometry of the holes. The shift gives a direct, non-destructive measure of wear.

References

Aminzadeh, A., Dimitrova, M., Meiabadi, M.S., Karganroudi, S.S., Ibrahim, H., Non-contact inspection methods for wind turbine blade maintenance: techno–economic review of techniques for integration with industry 4.0, Journal of Nondestructive Evaluation 42, 67 (2023). https://doi.org/10.1007/s10921-023-00967-5

Anstis, G.R., Chantikul, P., Lawn, B.R., Marshall, D.B., A Critical Evaluation of Indentation Techniques for Measuring Fracture Toughness: I, Direct Crack Measurements, Journal of the American Ceramic Society 64, 533-538 (1981). https://doi.org/10.1111/j.1151-2916.1981.tb10320.x

Barlet, M., Delaye, J., Charpentier, T., Gennisson, M., Bonamy, D., Rouxel, T., Rountree, C. L., Hardness and toughness of sodium borosilicate glasses via Vickers's indentations, Journal of Non-Crystalline Solids, Volumes 417–418, 66-79 (2015). https://doi.org/10.1016/j.jnoncrysol.2015.02.005

Blasse, G, Grabmaier, B.C., Luminescent Materials, Springer, Berlin (1994)

Chehrehzad, M., Kecibas, G., Besirova, C., Uresin, U., Irican, M., Tool wear prediction through AI-assisted digital shadow using industrial edge device, Journal of Manufacturing Processes 110, 110-124 (2024). https://doi.org/10.1016/j.jmapro.2024.01.052

Daily, J., Peterson, J., Predictive maintenance: How big data analysis can improve maintenance, In: Supply Chain Integration Challenges in Commercial Aerospace, pp. 267-278, Springer (2017). https://doi.org/10.1007/978-3-319-46155-7_18

Diamanti, E., Iriarte, E., Oblak, E., Domínguez-Meister, S., Ibáñez, I., Use of smartphones as optical metrology tools for surface wear detection, The International Journal of Advanced Manufacturing Technology 114, 2847-2860 (2021). https://doi.org/10.1007/S00170-021-06840-X

Dieke, G.H., and Crosswhite, H.M., The Spectra of the Doubly and Triply Ionized Rare Earths, Applied Optics 2, 675-686 (1963). https://doi.org/10.1364/AO.2.000675

Fan, H., Del Campo, L., Montouillout, V., Malki, M., Ionic conductivity and boron anomaly in binary lithium borate melts,

Journal of Non-Crystalline Solids, Volume 543, 120160 (2020). https://doi.org/10.1016/j.jnoncrysol.2020.120160.

Ogunnowo, E.O., Adewoyin, M.A., Fiemotongha, J.E., Igunma, T.O., Adeleke, A.K., Systematic Review of Non-Destructive Testing Methods for Predictive Failure Analysis in Mechanical Systems, Iconic Research And Engineering Journals, Volume 4, Issue 4 (2020) Page 207-222. https://www.irejournals.com/paper-details/1708638

Galarza-Urigoitia, N., Rubio-García, B., Gascón-Álvarez, J., Aznar-Lapuente, G., Olite-Biurrun, J., Predictive maintenance of wind turbine low-speed shafts based on an autonomous ultrasonic system, Engineering Failure Analysis 104, 308-320 (2019). https://doi.org/10.1016/J.ENGFAILANAL.2019.04.048

Moreira, E.E., Alves, F.S., Martins, M., Ribeiro, G., Pina, A., Industry 4.0: Real-time monitoring of an injection molding tool for smart predictive maintenance, In: 2020 25th IEEE International Conference on Emerging Technologies and Factory Automation (ETFA), Vol. 1, pp. 1209-1212, IEEE (2020). https://doi.org/10.1109/ETFA46521.2020.9212167

Rimbach, A.C., Steudel, F., Ahrens, B., Schweizer, S., Tb^{3+}, Eu^{3+}, and Dy^{3+} doped lithium borate and lithium aluminoborate glass: Glass properties and photoluminescence quantum efficiency, Journal of Non-Crystalline Solids 499, 380-386, (2018). https://doi.org/10.1016/j.jnoncrysol.2018.07.029

Shelby, J.E., Introduction to Glass Science and Technology, Royal Society of Chemistry, 2005

Swain, A., Khasnobish, A., Rani, S., Bhaumik, C., Chakravarty, T., MilliWear — A Short Range InSAR Approach for Surface Wear Inspection using mm-Wave Radar, In: 2022 IEEE SENSORS, pp. 1-4, IEEE (2022). https://doi.org/10.1109/SENSORS52175.2022.9967307

Challenging Glass Conference Proceedings – Volume 10 – June 2026 – Louter, Bos & Belis (Eds.)
International Conference on the Architectural and Structural Application of Glass
Challenging Glass Conference 10 – 15-17 June 2026 – TU Delft – The Netherlands

Platinum Sponsor

SAINT-GOBAIN

Gold Sponsors

EASTMAN

kuraray

NorthGlass®

sedak

seele

Silver Sponsors

DOW®

octatube

PERMASTEELISA GROUP

SEEN

Organisation

TU Delft

Technische Universität München

GHENT UNIVERSITY